Gas-solid Contact in Fluidized Beds

C. Y. Shen and H. F. Johnstone, University of Illinois, Urbana, Illinois

According to the concept of two-phase fluidization, a part of the gas in a fluidized reactor passes through the uniform dispersed solid-gas phase in the form of bubbles, channels, and slugs. Material transport by mixing or diffusion takes place at the phase boundaries. A mass transfer coefficient between the two phases may be used to evaluate the effectiveness of contact between the gas and solid. The reaction rate for the catalytic decomposition of nitrous oxide was determined in a fluidized bed of impregnated alumina particles and compared with the corresponding rate in a fixed bed. Simultaneous rate equations were established based on the assumption that the continuous phase is either completely unmixed or uniformly mixed, and the discontinuous phase passes without mixing. The effects of the velocity of the gas, the particle size, and the bed depth on the transfer coefficient were investigated. Applications to heat transfer in fluidized beds and equipment design are discussed.

In a dense-phase fluidized reactor the gas stream may be considered to exist in two phases, according to the concept proposed by Toomey and Johnstone(*8*). The continuous phase comprises a uniform mixture of a part of the gas which supports the solid particles and flows through the bed at the same velocity as that at incipient fluidization. The excess gas which moves through the bed as bubbles, slugs, and channels is the discontinuous phase. Since the solid particles are for the most part retained in the continuous phase, the reactants in the discontinuous phase must be transferred to the continuous phase before they can react with the solid. This concept provides a simple model for the reaction mechanism in a fluidized bed. In a previous paper(*3*) the part of the reaction rate above that at incipient fluidization was attributed to the presence of the discontinuous phase and was correlated with the gas velocity and particle size by analogy with the pressure-drop relationship(*8*).

Although the mechanism of the formation of bubbles and their behavior in the fluidized bed is not entirely clear, the rate of transfer between the two phases may be expressed in terms of a coefficient which depends on such factors as the rate of gas flow, size of the particles, and depth of the bed. The transfer coefficient is a measure of the intimacy of the gas-solid contact in fluidized beds and should be useful in the design of fluidized reactors. Its value can be calculated from data on reaction kinetics in a fluidized bed by comparison with corresponding data for a fixed bed, a suitable model being used as a basis for establishing the simultaneous rate equations. The following models have been used for the present calculations.

C. Y. Shen is at present with Monsanto Chemical Company, Dayton, Ohio.

Consecutive Mass Transfer and Reaction

The fluidized bed is considered to be comprised of two fluid phases: a gas-solid mixture and a pure gas phase, analogous to a liquid with gas bubbles. For a first-order reaction, assuming that mixing within each phase is negligible, the mass transfer coefficient can be calculated from two simultaneous first-order linear differential equations obtained from a material balance on each phase.

$$\frac{dC_d}{d\theta} = -k_d(C_d - C_c) \quad (1)$$

$$\frac{dC_c}{d\theta} = -k_c C_c - \frac{\theta_d V_d}{\theta_c V_c}\frac{dC_d}{d\theta} \quad (2)$$

where k_d is the transfer coefficient expressed as moles per unit time per unit volume of bed per unit concentration difference between the two phases. This definition is similar to the capacity coefficient for an adsorption tower, which is characteristic of the equipment design. k_c is the first-order reaction rate constant. Since the velocity of the gas is different in the two phases, in order to transform Equations (1) and (2) to distance coordinates the time of detention must be introduced.

$$\frac{dC_d}{dz} = -\frac{\theta_d k_d}{L}(C_d - C_c) \quad (3)$$

$$\frac{dC_c}{dz} = \frac{V_d}{V_c}\frac{\theta_d}{L}k_d(C_d - C_c) - \frac{\theta_c k_c C_c}{L} \quad (4)$$

The solution of Equations (3) and (4) is

$$C_d = A_1 e^{\frac{R_1 z}{L}} + B_1 e^{\frac{R_2 z}{L}} \quad (5)$$

$$C_c = A_2 e^{\frac{R_1 z}{L}} + B_2 e^{\frac{R_2 z}{L}} \quad (6)$$

where

$$R_1 = \frac{1}{2}\left[-b + \sqrt{b^2 - 4c}\right],$$

$$R_2 = \frac{1}{2}\left[-b - \sqrt{b^2 - 4c}\right],$$

$$b = k_d\theta_d\left(\frac{V}{V_c}\right) + k_c\theta_c,$$

$$c = k_c k_d \theta_d \theta_c$$

The arbitrary constants A_1, A_2, B_1, and B_2 can be evaluated from the boundary conditions:

$$\text{At } z = 0,\ C_d = C_c = C_1, \text{ and } \frac{dC_c}{dz} = -\frac{k_c C_1 \theta_c}{L} \quad (7)$$

Therefore,

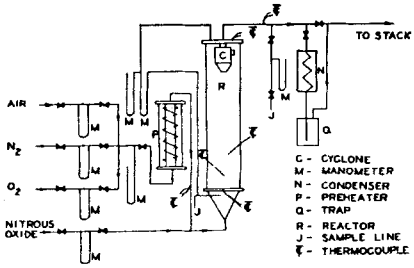

Fig. 1. Diagram of apparatus.

$$\frac{C_d}{C_1}=\frac{1}{R_1-R_2}\left[R_1 e^{\frac{R_2 z}{L}}-R_2 e^{\frac{R_1 z}{L}}\right] \quad (8)$$

$$\frac{C_c}{C_1}=\frac{1}{R_1-R_2}\left[(R_1+k_c\,\theta_c)\,e^{\frac{R_2 z}{L}}-(R_2+k_c\,\theta_c)\,e^{\frac{R_1 z}{L}}\right] \quad (9)$$

Furthermore, from a material balance at the outlet

$$\frac{C_2}{C_1}=\frac{V_c}{V}\left(\frac{C_c}{C_1}\right)+\frac{V_d}{V}\left(\frac{C_1}{C_d}\right) \quad (10)$$

The subscripts 1 and 2 denote the inlet and outlet conditions, respectively. Since C_2/C_1 is measured directly and k_c is known from fixed-bed studies, the value of k_d can be calculated from Equations (8) to (10).

Continuous Reactor Model

The continuous phase is assumed to be equivalent to a well-stirred reactor of constant and uniform composition at a fixed gas velocity. When steady state exists, the amount of reactants flowing into the reactor will equal the amount that flow out plus those that react.

$$Q_c\frac{dC_c}{d\theta}=0=V(C_1-C_2)-Q_c\,k_c\,C_c \quad (11)$$

where Q_c = volume of the continuous phase $= V_c\theta_c$
or

$$C_c=\frac{V}{k_c\,V_c\,\theta_c}(C_1-C_2) \quad (11a)$$

From Equation (1)

$$k'_d=-\frac{1}{\theta_d}\ln\left[\frac{C_{d2}-C_c}{C_{d1}-C_c}\right] \quad (12)$$

k'_d is the transfer coefficient for the continuous reactor model.

Table 1.—Gas Rates at Minimum Fluidization and Incipient Formation of Two Phases

Catalyst size, mesh	Temperature of air, °F.	Minimum fluidization rate, std. cu. ft./min.	Incipient two-phase fluidization rate, std. cu. ft./min.
165–200	800	0.043	0.059
165–200	750	0.046	0.063
165–200	700	0.049	0.068
120–165	800	0.069	0.105
120–165	750	0.074	0.112
120–165	700	0.080	0.121
60–120	800	0.107	0.149
60–120	750	0.114	0.159
60–120	700	0.123	0.171

The concentration of the reactants in the discontinuous phase at the outlet can be obtained from the material balance at the exit

$$C_{d2}=\frac{1}{V_2}(VC_2-V_c\,C_c) \quad (13)$$

The retention time in the discontinuous phase can be estimated from the bed expansion,

$$\theta_d=A\,(L_f-L_{mf})\,/\,(V-V_c) \quad (14)$$

The value of k'_d can be found from Equations (11) to (14)

EXPERIMENTAL

The reaction chosen for study was the catalytic decomposition of nitrous oxide, because the analysis is simple and the catalyst activity remains substantially constant over a long period of time. The rate of decomposition was measured in fixed and fluidized beds in the temperature range from 650° to 800°F. Nitrogen, air, or oxygen streams containing 1 to 2.5% nitrous oxide were used.

The kinetics of the reaction are discussed by Schwab and coworkers (*5* and *6*). Damköhler and Delcker (*1*) studied the decomposition in fixed beds of cupric oxide, alumina and alumina impregnated with cupric oxide, at various flow rates in the region of laminar flow. The reaction is first order and the yield depends on the time of contact and not on the linear velocity; hence the diffusional resistance is not a controlling step.

Apparatus. A diagram of the apparatus is shown in Figure 1. The individual gases were passed through filters, pressure regulators, and flow meters. The reactor was 4½ in. I.D. and 43 in. high and was made of 310 stainless steel. One thermocouple was embedded in the porous stainless steel support plate and two others were mounted through the column wall in the fluidized bed itself.

The reactor was heated electrically by chromel resistance ribbon which was wound in three sections around the reactor. The temperatures of the bottom and top sections were controlled manually with variable transformers, and the temperature of the middle section, which covered the entire catalyst bed, was regulated with an automatic controller.

The preheater was also made of a section of the 4½-in. stainless steel tubing 30 in. long. To secure high rates of heat transfer, the preheater was heated by both internal and external electric elements with variable inputs to keep the inlet gas at the desired temperature.

Sample lines were provided beneath the porous plate and at the top of the reactor. The pressure drop across the catalyst bed and the pressure inside the reactor were measured through pressure taps connected to manometers with ¼-in. copper tubing.

Catalyst. The catalyst was made by mixing 10 kg. of Alcoa XF-21-Si fluid cracking catalyst with 2.5 liters of solution containing 1 kg. of manganous nitrate and 350 g. of bismuth nitrate, drying for 5 days in a steam-heated vacuum oven, and finally roasting at 375°C. for 48 hr. in an electric furnace. The catalyst was separated into three fractions, 165-200, 120-165, and 60-120 mesh. by standard Tyler screens. The size distribution and composition of the catalyst are reported in a previous paper (*3*). The catalyst particles were generally round but not truly spherical.

Procedure. Air was used to fluidize the bed while the reactor was being heated to the desired temperature. After 8 to 12 hr. the reacting gas stream was passed into the apparatus and allowed to flow for 2 hr. at the set conditions. A sample of the exit gas was then taken for infrared analysis. The glass analysis cell, equipped with rock-salt-crystal windows, was flushed out thoroughly while the gas pressure was maintained at 800 mm. before adjustment to the final conditions of 72°F. and 745 mm. Temperatures, pressures, and flow rates were recorded during the sampling period.

Gas Analysis. The gas was analyzed for nitrous oxide in a Perkin-Elmer double-beam infrared spectrometer using the base-line technique de-

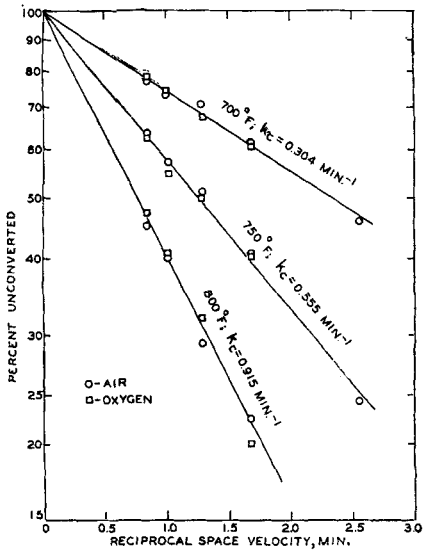

←Fig. 2. Decomposition rate of nitrous oxide in fixed beds: 2 kg. catalyst, 165-200 mesh; inlet-gas concentration, 1% nitrous oxide.

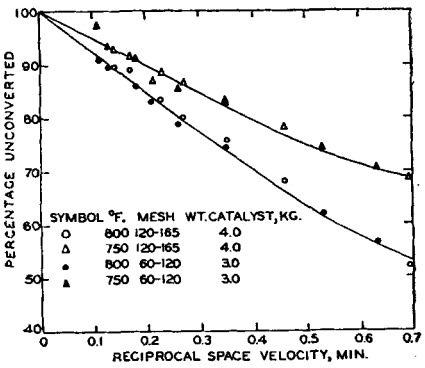

←Fig. 3. Decomposition rate of nitrous oxide in fluidized beds: inlet-gas concentration, 1% nitrous oxide.

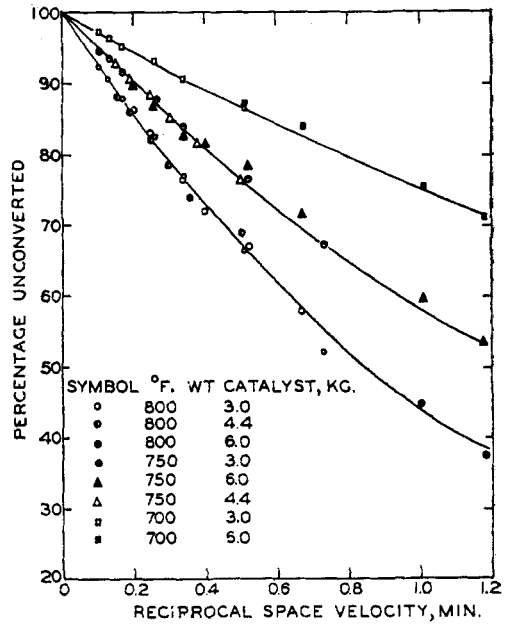

→Fig. 4. Decomposition of nitrous oxide in fluidized beds: effect of temperature and bed depth; inlet-gas composition, 1% nitrous oxide.

scribed by Wright(*11*). The wave number used was 2,180 cm.$^{-1}$

RESULTS

The results with air and oxygen as the diluent gases in the fixed-bed reactor at different temperatures are shown in Figure 2. The reciprocal space velocity shown is the ratio of the volume of the catalyst particles to the volumetric gas-feed rate at standard conditions. The volume of the particles was calculated from the weight of catalyst and the absolute particle density.

The initial nitrous oxide concentration does not affect the fractional rate of decomposition, and the reaction must follow a first-order mechanism. When nitrogen was used instead of air or oxygen, the reaction rate was slightly higher. The probable explanation is that oxygen decreases the number of anion vacancies on the catalyst surface and thus reduces the activity of the catalyst(*9*). The activation energies, calculated from the effect of temperature according to the Arrhenius equation, for the nitrogen and air or oxygen series are about the same, 17 kcal./g.mole. The effect of bed depth and particle size on the decomposition rate in fixed beds is small. The effects of temperature, particle size, and bed depth on the over-all reaction rate in fluidized beds of the same catalyst, with air as the diluent gas, are shown in Figures 3 and 4. The reaction rate in general is lower than that in fixed beds.

The minimum gas rate at which fluidization takes place was determined from the pressure-drop measurements. This was taken as the intersection of the straight lines for the fixed- and fluidized-bed regions in the pressure-drop vs. gas-velocity plots. In a previous paper(*8*) the relation between gas velocity and pressure drop was expressed by

$$\frac{\Delta P_{ke}}{\Delta P_{mf}} = (lD_p^{0.5} - m) \ln \frac{V}{V_v} \quad (15)$$

The incipient two-phase fluidization rate was obtained from the intercept of the straight line on the plot of $\Delta P_{ke}/\Delta P_{mf}$ vs. log V. The results are shown in Table 1.

The expansion of the bed during fluidization was measured in a 3.75-in. I.D., 40-in.-long glass column. Lewis, and Bauer(*4*) have shown that the fractional increase in height above that at minimum fluidization is proportional to the increase in the superficial gas velocity above that at incipient fluidization. This relationship can be expressed by

$$\frac{(L_f - L_{mf})}{L_{mf}} = \frac{0.0188}{D_p^{0.5}} (u - u_v) \quad (16)$$

This equation was used to calculate the height of the fluidized bed at any gas velocity.

TRANSFER COEFFICIENTS

The transfer coefficient between the two phases can be calculated from either of the two models presented above, together with the reaction-rate data in the fixed and fluidized beds. The reaction-rate constant for the fixed bed does not change under isothermal and isobaric conditions. Deviation from this value in the fluidized bed is caused by the presence of the discontinuous phase, and the transfer coefficient can be calculated as follows:

Consecutive Transfer and Reaction Steps. Since the coefficient cannot be expressed explicitly from Equations (8) to (10), its value must be calculated by a trial-and-error method. A value of k_d was first assumed and the outlet concentration was calculated from these equations. The calculated result was then compared with the experimental value and the value of k_d changed until the agreement was good. The values of k_d found by this method varied over a tenfold range from 9.6 to 98.8 min.$^{-1}$ depending on the gas velocity, bed depth, catalyst size, and temperature(*7*).

When the catalyst size is small compared with the diameter of the reactor, dimensional analysis shows that the variables that affect the transfer coefficient can be grouped as follows:

$$\frac{u}{k_d D_p} = \rho \left[\left(\frac{D_p u \rho_g}{\mu} \right) \left(\frac{L}{D_T} \right) \right.$$

$$\left(\frac{\rho_s - \rho_g}{\rho_g}\right)(\epsilon)\Bigg] \qquad (17)$$

In the range studied the gas density, 0.032 to 0.034 lb./cu.ft., had no noticeable effect on the group u/k_dD_p, which may be regarded as a modified Peclet number. The effects of gas velocity, bed depth, and particle size are shown in Figures 5 and 6. Since both the bed expansion and void fraction are functions of gas velocity, the effect of bed depth on the value of the transfer coefficient can be seen from the logarithmic plot of u/k_dD_p vs. gas velocity in Figure 5. The effect of gas velocity on the Peclet number increases with the height-diameter ratio. A possible explanation for this is that there is a greater tendency for channeling, or slugging, with coalescence of bubbles, which affects the gas-flow pattern in deep beds. This decreases the contact between the two phases and lowers the transfer coefficient.

Figure 6 shows that the Peclet number increases with increase in particle size of the catalyst. The average value of k_d for each series of runs is directly proportional to the bed depth and is roughly inversely proportional to the particle diameter. This indicates that k_d is a function of the total surface area of the particles and that the group uL/k_dD_T can be used to correlate all the data involving these variables such as temperature, particle size, and bed depth. This correlation is shown in Figure 7.

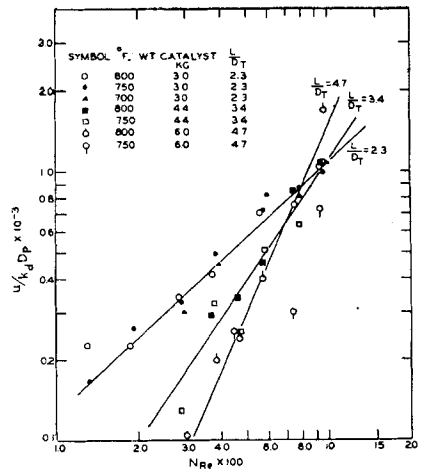

Fig. 5. Effect of bed depth on modified Peclet number: catalyst size, 165-200 mesh.

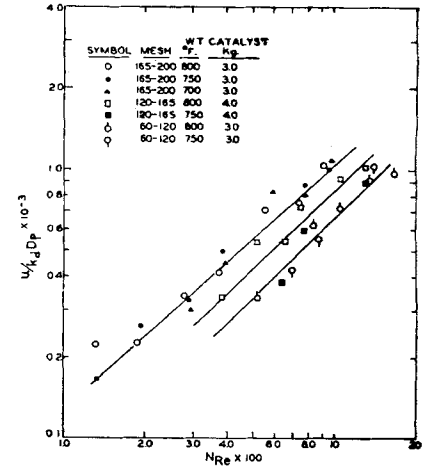

Fig. 6. Effect of particle size on modified Peclet number.

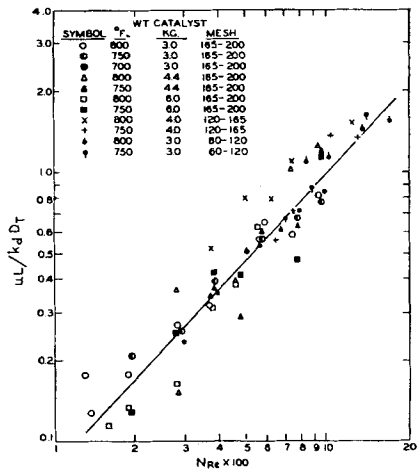

Fig. 7. Correlation of transfer coefficients based on model for consecutive transfer and reaction.

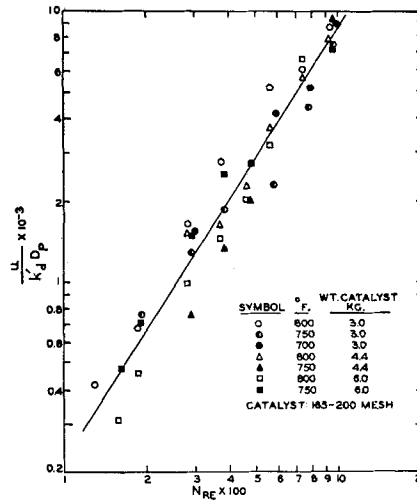

Fig. 8. Correlation of transfer coefficients based on continuous-reactor models.

Continuous Reactor Model. The advantage of the continuous reactor model for representing the fluidized system is that it is simpler to use for higher order reactions and the result on a small unit should be useful for predicting the performance of larger reactors. For the present study a reaction-rate constant calculated from the conversion rate at incipient two-phase fluidization was used to calculate k'_d according to Equations (11) to (14). The modified Peclet number for the continuous reactor model u/k'_dD_p is plotted against the Reynolds number in Figure 8. In this case the data points fall along the line with a slope of 1.6.

Each experimental value of k_d and k'_d was obtained from an average of two or three runs to minimize the fluctuations caused by the unsteadiness of the bed, since a slight error in the outlet concentration was sufficient to introduce a large error in the calculated transfer coefficient. In a few cases, especially at low temperatures, nitrous oxide decomposed in the fluidized bed at high gas velocities was apparently less than that at incipient fluidization, and the transfer coefficient could not be calculated.

DISCUSSION

Although either the consecutive transfer model or the continuous reactor model can be used for higher order catalytic or homogeneous reactions, the difficulty in using the former lies in the fact that the differential equations become nonlinear. The boundary conditions are known at one end, however, and a solution of the equations can be obtained by a digital computer or by a series solution (7). Since the transfer coefficient does not depend on the reaction order, the value obtained from a first-order reaction should hold for the higher order reactions.

The models and concepts developed for reactions in the fluidized reactor can be applied to heat and mass transfer processes. Experimental measurements of the rate of heat and mass transfer between gas and solid particles in fluidized beds are difficult to make since shallow beds must be used because of the high values of the coefficients. Such fluidized beds behave entirely differently from those used for dense-phase fluidization. Wamsley and Johanson (10) used a transient heating method with beds less than 3 in. deep to determine the heat transfer coefficient between fluidized solids and gas. Their results have been recalculated on the basis of consecutive transfer stops according to the

TABLE 2.—HEAT TRANSFER COEFFICIENTS CALCULATED FROM DATA OF WAMSLEY AND JOHANSON (*10*)

Run	Inlet temp., °F	Time, hr.×10³	Outlet temp., °F.	T_{p1}, °F.	N_{Re}	h_d B.t.u. (hr.)(°F.)(sq.ft.), obs.	$\frac{\rho_g C_p}{aA} k_d$ B.t.u. (hr.)(°F.)(sq.ft.), calc.
a. 100-115 mesh							
GA12	137.0	90 3	119.9	94.1	1.12	0.0056	0.0292
GA21	137.9	65.0	122.3	98.3	1.86	0.0107	0.0276
GA14	142.1	58.6	128.6	110.2	2.68	0.0215	0.0267
GA17	138.7	62.8	126.3	113.2	3.34	0.0348	0.0260
b. 60-65 mesh							
GA18	138.7	62.2	119.9	101.0	2.93	0.0185	0.0251
GA10	140.8	48.9	124.3	107.1	4.25	0.0326	0.0240
GA13	139.9	47.5	124.3	109.8	5.37	0.0523	0.0235
GA20	139.0	48.3	126.3	114.0	6.43	0.0621	0.0229
c. 32-35 mesh							
GA11	137.2	32.8	113.6	99.8	8.97	0.0197	0.0248
GA16	141.8	44.5	124.3	113.9	11.31	0.0525	0.0230
GA15	139.0	37.8	122.3	111.4	13.25	0.0797	0.0228
GA19	139.4	33.4	122.3	114.5	16.08	0.1850	0.0223

two-phase theory.

From a heat balance the rate of change of temperature of the gas with distance through the bed is given by

$$-w_d C_p \frac{dT_d}{dz} - A\, a\, h_d (T_d - T_c) \tag{18}$$

$$-w_c C_p \frac{dT_c}{dz} = w_d C_p \frac{dT_d}{dz} + h_c a A (T_c - T_p) \tag{19}$$

The time required to bring the temperature of the solid to equilibrium with the gas is very short, as indicated by the experimental results of Johnstone, Pigford, and Chapin(*2*) on heat transfer to clouds of particles. It may be assumed, therefore, that the temperature of the gas in the continuous phase is essentially equal to the particle temperature T_p. This is equivalent to saying that the heat transfer coefficient h_c between particle and gas approaches infinity. The solid particles have a much higher heat capacity than the gas and they mix rapidly; thus the temperature of the solid may be assumed to be constant throughout the bed. With these assumptions, the coefficient h_d can be obtained from the following equations.

$$h_d = \frac{w_d C_p}{a A L} \ln \frac{T_1 - T_p}{T_{d2} - T_p} \tag{20}$$

$$T_{d2} = \frac{w}{w_d} T_2 - \frac{w_c}{w_d} T_p \tag{21}$$

$$T_p = T_{p1} + \frac{1}{w_s C_s} \int_o^\theta w C_p (T_1 - T_2)\, d\theta \tag{22}$$

The inlet temperature T_1 is the corrected value after adjustment for the heat losses, as suggested by Wamsley and Johanson. The temperature of the particles was calculated from Equation (22) by graphical integration of the published data. The time θ was chosen as that at the middle of a run. The values calculated for h_d are listed in Table 2.

When heat or mass is transferred by means of fluid motion near the boundary of the two phases, the same mechanism controls both processes. Therefore, it is reasonable to assume that the rate of heat transfer under a temperature gradient and the rate of mass transfer under a concentration gradient can be correlated by the following equation:

$$h_d = \beta \frac{\rho_g C_p}{a A} k_d \tag{23}$$

where β is a proportionality constant nearly equal to unity. The value of the group $\rho_g c_p k_d / aA$, in which k_d is determined from Figure 7 by extrapolation, is also listed in Table 2.

It is to be noted that h_d increases with the gas velocity (it is proportional to $u^{1.6}$); whereas k_d is affected only slightly by velocity. For the smaller particle sizes, 110-115 and 60-65 mesh, the value of h_d follows a similar inverse function of the particle diameter, as shown for k_d in Figure 6, but this is not true for the series of 32-35 mesh size at low velocities. These differences may be due to an error in the assumption of uniform temperature of the solid particles. The large dependence of h_d on velocity may also be a result of using very shallow beds. The agreement of the calculated data with the experimental results, however, is sufficient to show that the concepts of the fluidized bed are useful and approximately correct. Thus the rate of heat transfer between the two phases is the rate-determining step. In practice a greater rate of heat transfer between the gas and particles will be obtained with smaller particles, but more of the gas will pass through the bed as the discontinuous phase. Thus there is a particle size at which the over-all rate of transfer is maximum. The optimum size will also depend on other factors such as the fluidization rate, reaction rate, heat transfer from the wall, etc., which affect economical considerations.

CONCLUSIONS

A fluidized catalyst bed may be considered to be composed of two phases, a continuous phase and a discontinuous phase. In the continuous phase the particles are supported by the gas stream moving at the same velocity as that at incipient fluidization. In the discontinuous phase the excess gas moves through the bed in the form of bubbles, slugs, or channels. In the presence of the discontinuous phase the reactant, for the most part, must be transferred to the continuous phase before reaction can occur. The increase of the over-all reaction rate above that at incipient two-phase fluidization may be attributed to the effect of gas velocity on the mass transfer between the two phases.

From measurements of the catalytic decomposition rate of nitrous oxide, on the assumption that both phases are unmixed, the transfer coefficient was found to be inversely proportional to the particle size. The effect of gas velocity on the transfer coefficient depends very much on the bed depth. The transfer coefficients were also calculated from published data on heat transfer. The approximate agreement between the calculated and observed values shows that the proposed model is sound.

Since the total rate of conversion in a fluidized reactor depends on the transfer rate and the reaction rate in the continuous phase, the rate-determining step evidently depends on the relative magnitude of these rate coefficients. Measurement of the transfer coefficient should enable design calculations and evaluation of the optimum conditions to be made from fixed-bed studies.

NOTATION

a = surface area of particles per unit volume, sq.ft/cu.ft.
A = a constant; area of the reactor, sq.ft.
B = a constant
C = concentration, moles/cu.ft.
C_p = specific heat of gas, B.t.u./(lb.)(°F.)
C_s = specific heat of solid, B.t.u./(lb.)(°F.)
D_p = particle diameter, ft.
D_T = reactor diameter, ft.
h = heat transfer coefficient, B.t.u./(hr.)(°F.)(sq.ft.)
k_d = transfer coefficient for consecutive model, min.$^{-1}$
k'_d = transfer coefficient for continuous model, min.$^{-1}$
k_c = first-order reaction-rate constant, min.$^{-1}$
L = height of bed, ft.
l, m = constants
ΔP_{mf} = pressure drop at minimum fluidization, in. of water
ΔP_{ke} = pressure drop above ΔP_{mf}, caused by kinetic energy losses, in. of water
N_{Re} = Reynolds number, $D_p u \rho_g/\mu$, dimensionless
Q = volume of bed, cu.ft.
T = temperature, °F.
u = linear gas velocity, ft./sec.
V = volumetric gas velocity, cu.ft./min.
w = mass rate of flow of gas, lb./hr.
z = length coordinate, ft.

Greek Letters

β = constant
ε = porosity
θ = time, min.
μ = viscosity, lb./(ft.)(sec.)
ρ = density, lb./cu.ft.

Subscripts

1 = inlet condition
2 = outlet condition
c = continuous phase
d = discontinuous phase
f = fluidization condition
g = gas
s = solid
v = incipient two-phase fluidization
mf = minimum fluidization
ke = kinetic energy

LITERATURE CITED

1. Damköhler, G., and G. Delcker, *Z. Elektrochem.*, 44, 193 (1938).
2. Johnstone, H. F., R. L. Pigford, and J. H. Chapin, *Trans. Am. Inst. Chem. Engrs.*, 37, 95 (1941).
3. Johnstone, H. F., J. D. Batchelor, and C. Y. Shen, *A.I.Ch.E. Journal*, 1, 318 (1955).
4. Lewis, W. K., E. R. Gilliland, and W. C. Bauer, *Ind. Eng. Chem.*, 41, 1104 (1949).
5. Schwab, G. M., and H. Schultes, *Z. physik. Chem.*, **B9**, 265 (1930).
6. Schwab, G. M., and G. Stager, *Z. physik. Chem.*, **B25**, 418 (1934).
7. Shen, C. Y., Ph.D. thesis, Univ. Illinois (1954); microfilm copies from University Microfilms, Inc., Ann Arbor, Michigan.
8. Toomey, R. D., and H. F. Johnstone, *Chem. Eng. Progr.*, 48, 220 (1952).
9. Wagner, C., *J. Chem. Phys.*, 18, 69 (1950).
10. Wamsley, W. W., and L. N. Johanson, *Chem. Eng. Progr.*, 50, 347 (1954).
11. Wright, N., *Ind. Eng. Chem., Anal. Ed.*, 13, 1 (1941).

Presented at the A.I.Ch.E. Houston meeting

Prediction of Ternary Vapor-liquid Equilibria from Boiling-point Data

Mitsuho Hirata, Tokyo Institute of Technology, Tokyo, Japan

A knowledge of ternary vapor-liquid equilibrium relations is indispensable to the design of columns for ternary rectification as well as azeotropic and extractive distillations. To determine these relations experimentally requires very involved analyses. It is, therefore, highly desirable to estimate ternary equilibrium relations without those analyses and, better still, without experimentation.

Attempts have been made to predict the ternary vapor-liquid equilibria on the theoretical basis of thermodynamic relations among activity coefficients of three components and by use of three binary equilibrium relations available for three combinations of components from Carlson and Colburn (*3*), Benedict, Johnson, Solomon, and Rubin (*1*), Colburn and Schoenborn (*4*), White (*20*), Wohl (*21*), Redlich and Kister (*16*), and Edwards, Hashmall, Gilmont, and Othmer (*6*). Some of these give good estimations for certain ternary systems but fail in other systems or are laborious to calculate accurately.

Scheibel and Friedland (*17*) proposed an empirical method which gives good agreement with many observed data; however, it is lacking in theoretical background and requires different procedures of calculation for different types of ternary systems concerned.

Othmer, Ricciardi and Thaker (*15*) derived a fundamental thermodynamic equation for ternary systems and used it for checking the vapor-liquid equilibrium data available for a ternary system.

PREDICTION FROM TEMPERATURE-COMPOSITION DATA

A method is here presented for estimating vapor compositions at constant-pressure equilibrium from boiling-point data of ternary systems. This method requires the boiling-point–composition data of the system, but the experimental procedures for determining boiling points of definite ternary liquid mixtures are generally much simpler than those required for determining entire vapor compositions of the system.

The method offered for ternary systems is a natural extension of the method for binary systems developed by the author (*8*) and Othmer, Ricciardi, and Thaker (*15*). It is based on the linear property of the equilibrium relations when